Tmem27 dimerization, deglycosylation, plasma membrane depletion, and the extracellular Phe-Phe motif are negative regulators of cleavage by Bace2

Daria Esterházy^{1,2}, Pinar Akpinar^{3,a} and Markus Stoffel^{1-4,*}

¹ Institute of Molecular Systems Biology, ETH Zurich, Wolfgang-Pauli Strasse 16, CH-8093 Zurich, Switzerland

- ²Competence Centre for Systems Physiology and Metabolic Diseases, ETH Zurich, CH-8093 Zurich, Switzerland
- ³ Rockefeller University, 1230 York Avenue, New York, NY 10065, USA
- ⁴ Faculty of Medicine, University of Zurich, CH-8091 Zurich, Switzerland
- *Corresponding author e-mail: stoffel@imsb.biol.ethz.ch

Abstract

The pancreatic β-cell surface protein Tmem27 is promotes the preservation of functional β-cell mass. It is a selective substrate of the protease Bace2, yet the intramolecular features of Tmem27 that regulate its processing by this sheddase have not been characterized. In particular, the importance of homodimerization, glycosylation, trafficking to the plasma membrane (PM), the existence of multiple cleavage sites, and the amino acid residues that govern these features are currently unknown. Using Tmem27 mutational analysis and multiple biochemical approaches, we here show that Tmem27 dimerization is a dynamic process mediated by its intracellular cysteine residue and that prevents Tmem27 cleavage, that extracellular asparagine glycosylation is essential for Tmem27 trafficking to the PM and its processing by Bace2, that the amount of Tmem27 at the PM is proportional to its total cell levels upon glucose stimulation and Bace2 inhibition, and that the double phenylalanine motif in the Tmem27 cleavage site is an intramolecular Bace2 inhibitor. These findings define structural properties of Tmem27 that affect the susceptibility to its protease Bace2 and have implications for the efficiency with which Tmem27 and other Bace2 substrates are cleaved in normal and disease states.

Keywords: ectodomain cleavage; MIN6; pancreatic β -cell; protease inhibitor.

Introduction

Tmem27 is a highly abundant type I transmembrane protein that is enriched in the cell surface of pancreatic β -cells. In the past years, it has attracted increasing attention because of its ability to

^aPresent address: PriceSpective, 22 Tudor Street, London EC4Y 0AY, UK

promote β-cell proliferation and insulin secretion when overexpressed, two properties that would counteract the typical deficits of β cells in the course of type 1 and type 2 diabetes progression (Kahn et al., 2006) and raise the exciting possibility that Tmem27 could be targeted to treat these diseases. Recently, we have discovered that one way to increase endogenous Tmem27 levels and attain these beneficial effects is to inhibit its inactivating protease, Bace2 (Esterházy et al., 2011). The activity of this sheddase normally leads to the degradation of the 43-kDa fulllength (FL) Tmem27 protein to a 25-kDa N-terminal, shed fragment (NTF) that is released into the extracellular space and a 22-kDa C-terminal, membrane-bound fragment (CTF) that is further processed by y-secretase (Esterházy et al., 2011). However, Tmem27 is also observed as a dimer of 90 kDa (Akpinar et al., 2005), raising the question of whether dimer formation has an effect on the shedding by Bace2. Furthermore, Tmem27 has two predicted extracellular asparagine (N) glycosylation sites, a posttranslational modification that has been shown to be essential for proper trafficking of β-cell glucose transporter Glut2 (Ohtsubo et al., 2011) and therefore might affect the amount of Tmem27 that can interact with Bace2. Finally, the cleavage occurs at three proximal sites within the Tmem27 extracellular domain (Esterházy et al., 2011), yet it is unknown which of the sites is the most important for shedding by Bace2. As Tmem27 is the only known Bace2-selective substrate so far and given its medical potential, we sought to characterize the Tmem27 intramolecular determinants for dimerization, glycosylation, cell surface localization, and cleavage by Bace2. Using mutational analysis combined with multiple biochemical approaches, we found that monomeric but not dimeric Tmem27 is the substrate for Bace2, that normal N-glycosylation is required for the ability of Tmem27 to traffic to the cell surface and is essential for cleavage by Bace2, that high-glucose and Bace2 inhibition lead to increased levels of Tmem27 at the plasma membrane (PM), and that the double phenylalanine (Phe-Phe)-containing cleavage region of Tmem27 acts an intramolecular Bace2 inhibitor, whereas the most membrane proximal motif is the preferred Bace2 cleavage site.

Results

The intracellular cysteine of Tmem27 is essential for its dimerization but not cleavage by Bace2

Tmem27 forms homodimers that can be observed on Western blots of nonreduced mouse insulinoma (MIN6) cell line lysates (Akpinar et al., 2005). To determine which of the two, the monomer or the dimer of Tmem27, would accumulate upon Bace2 inhibition and thus be the likely substrate for the

protease, lysate from MIN6 cells treated with a Bace inhibitor (MerckBI) was analyzed under oxidizing conditions. Both the monomer and the dimer of Tmem27 were equally stabilized compared with vehicle control (Figure 1A). This suggested that either both are substrates or that only one oligomer is, but that the equilibrium between the two states is so dynamic that lack of Tmem27 cleavage would translate

into stability of the nonsubstrate as well. Interestingly, when γ -secretase, which normally removes the C-terminal fragment (CTF; Figure 1B) of Tmem27 generated by Bace2 cleavage, was inhibited with N-[N-(3,5-difluorophenacetyl)-L-alanyl]-S-phenylglycine t-butyl ester (DAPT; Esterházy et al., 2011), only a band corresponding to monomeric CTF was revealed under nonreducing conditions (Figure 1A), favoring

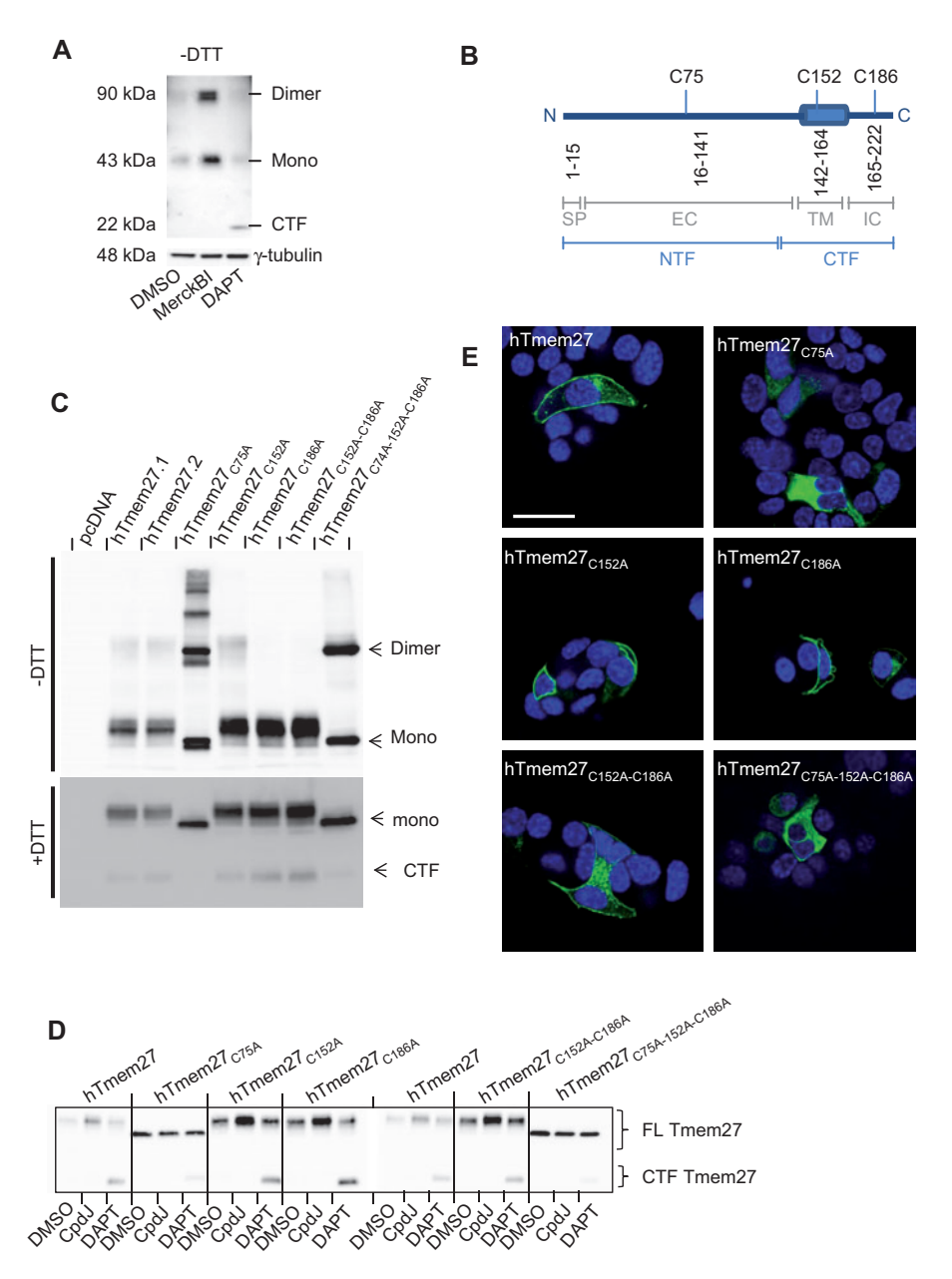


Figure 1 The intracellular cysteine of hTmem27 is essential for dimerization but not for cleavage by Bace2.

(A) Nonreducing (-DTT) Western blot for Tmem27 and γ-tubulin in lysates of MIN6 cells treated with DMSO, 5 μM MerckBI, or 1 μM DAPT for 6 h. Tmem27 dimer runs at 90 kDa, Tmem27 monomer (mono) runs at 43 kDa, monomeric Tmem27 CTF runs at 22 kDa. (B) Schematic representation of hTmem27 showing its topology, cleavage fragments as perceived by gel electrophoresis and positions of the three cysteine (C) residues. SP=signal peptide, EC=extracellular, TM=transmembrane, IC=intracellular, NTF=N-terminal fragment, CTF=C-terminal fragment. Numbers refer to hTmem27 amino acid residues. (C) Nonreducing (-DTT, top) and reducing (+DTT, bottom) Western blot for Tmem27 (α-V5) in lysates of MIN6 cells transfected with 5 μg of respective plasmid/106 cells 24 h before lysis. hTmem27.1 and hTmem27.2 represent transfections with two independent plasmid preparations. (D) Western blot for hTmem27 (α-V5) in lysates of MIN6 cells transfected with 5 μg of respective plasmid/106 cells 24 h before 16-h treatment with 1 μM DAPT, 200 nM CpdJ, or DMSO. (E) Immunofluorescence images of MIN6 cells transfected with 0.5 μg of respective plasmid/106 cells 24 h before fixation and staining for hTmem27 (α-V5). Bar=25 μM.

the concept that the monomer and not dimer is the substrate for Bace2.

Tmem27 has three conserved cysteine residues, one positioned extracellularly, C75 in human Tmem27 (hTmem27), one in the intramembrane domain, C152 in hTmem27, and one intracellularly, C186 in hTmem27 (Figure 1B). To assess which, if any, are involved in intermolecular Tmem27 disulfide bonds and could hence be used to determine the oligomerization state in which Tmem27 is a substrate for Bace2, the three residues of hTmem27 were mutated to alanine, individually, C152 and C186, or all three in one construct and transfected into MIN6 cells. Alanine was chosen over the more conservative serine residue as a substitution for C152 to avoid the insertion of a more charged side chain into the intramembrane domain that may affect membrane integration of the protein. The C75 and C186 residues were mutated to alanine for consistency between the mutants. Although mutating C75 and C152 did not prevent Tmem27 dimerization, the C186A mutation did, both in the single mutant and C152A-C186A-bearing construct of hTmem27 (Figure 1C). At the same time, the CTF was still observed. This suggests that the dimerization-deficient hTmem27C₁₈₆₄ is a monomeric substrate for Bace2. The C186A single mutant behaved as the wild-type construct; however, the C75A mutation resulted in a drastic biochemical phenotype, both in the single and in the triple cysteine mutant form: it appeared hyperoligomerized, ran at a lower molecular weight compared with the other constructs, and became visible as a sharp band following separation on a polyacrylamide gel, which suggested loss of glycosylation (Figure 1C). The C75A mutants also failed to display CTFs (Figure 1C), and similarly, no NTF could be detected in the supernatant of the cells (data not shown; see Figure 1B for position of NTF with respect to FL Tmem27). Analyzing the behavior of all the constructs expressed in MIN6 cells in the presence of a Bace inhibitor (CpdJ) revealed that all but the C75Acontaining constructs were strongly stabilized upon Bace2 inhibition and are thus substrates for this protease (Figure 1D). Upon addition of DAPT, a weak CTF could be detected for the C75A mutants, showing that a small fraction of the protein was still cleaved by Bace2 (Figure 1D). The inefficient cleavage of hTmem27C75A could be attributed to its increased dimerization; however, another possibility is that, given its altered glycosylation state, a mislocalization that prevents it from interacting with Bace2 at the PM and/or vesicles derived from it. Immunofluorescence analysis of MIN6 cells expressing the cysteine mutants revealed that indeed the latter was the case: while the C152A and C186A mutant localized to the PM as the wild-type construct, the C75A harboring constructs appeared diffuse and predominantly intracellular (Figure 1E). Taken together, these results show that monomeric Tmem27 is a substrate for Bace2.

Induced dimerization of Tmem27 prevents its shedding by Bace2

To further support the notion that dimeric Tmem27 is not a substrate for Bace2, an inducible dimer of Tmem27 was

generated by cloning FL hTmem27 or hTmem27-Δ171-222 (lacking the cytosolic domain including C186) N-terminal of a 10-kDa human FK506-binding protein (hFKBP) domain followed by an HA tag (ARIAD Argent homodimerization kit). The hFKBP protein dimerizes upon ligand binding, and the endogenous ligand can be replaced by synthetic high affinity ligands such as AP20817 (Jin et al., 2000). Furthermore, the hFKBP construct used harbored a F36V mutation (Fv) because this mutation augments the affinity of AP20817 for hFKBP ≈1000-fold. The FL hTmem27-Fv-HA construct behaved like hTmem27 without the FKBP fusion in terms of cleavage when expressed in MIN6 cells because the addition of Bace inhibitor (CpdJ) led to the stabilization of the FL protein and loss of CTF, whereas the addition of γ -secretase inhibitor DAPT stabilized its CTF (Figure 2A). Also, the NTF that is released upon Tmem27 cleavage by Bace2 was not detectable in the supernatant upon CpdJ addition (Figure 2B). The hTmem27- Δ 171-222-Fv-HA construct displayed a nonglycosylated pattern, was a poor Bace2 substrate based on the same assays (Figure 2A, b), and hence was not further considered as a useful tool to determine if the dimer of Tmem27 is Bace2 cleavage resistant. However, it was interesting to observe that although FL hTmem27-Fv-HA localized to the PM as expected, hTmem27-Δ171-222-Fv-HA (and Fv-HA empty vector) did not, a finding in line with the previous observation (Figure 1D, E) that glycosylation defects can result in Tmem27 mislocalization (Figure 2C).

Dimerizing FL hTmem27-Fv-HA in MIN6 cells by the addition of AP20817 led to the stabilization of FL protein in the cell lysate (Figure 2D, +DTT blot), which coincided with an enrichment of the dimer compared with extracts of vehicle control-treated cells (Figure 2D, -DTT blot). However, this total protein stabilization upon increased dimer formation was also observed for the non-Bace2 substrate constructs hTmem27-Δ171-222-Fv-HA as well as for the CTF of hTmem27-Fv-HA, raising the possibility that any AP20817-induced dimer is more resistant to protein turnover, also independently of Bace2 (Figure 2D). Similarly, the CTF of hTmem27-Fv-HA was stabilized upon AP20817 addition, and a 64-kDa band corresponding to the expected size of its dimer appeared (Figure 2D, -DTT blot), making either the FL or CTF levels ambiguous measures of Tmem27 accessibility to Bace2 in this setting. Yet, the fact that the NTF of Tmem27 was drastically decreased in the supernatant of hTmem27-Fv-HA-transfected MIN6 cells upon AP20817 addition (Figure 2D, top blot) strongly suggested that dimerization inhibited ectodomain shedding. The FL hTmem27-Fv-HA protein still localized to the MIN6 cell surface upon AP20817 addition to the cell culture medium (Figure 2E), ruling out that this lack of cleavage was due to mislocalization - which had correlated with the cleavage resistance of all the glycosylation defective constructs. These data show that the Tmem27 dimerization prevents its cleavage by Bace2 and further strengthen the above finding that monomeric Tmem27 is the substrate for the protease.

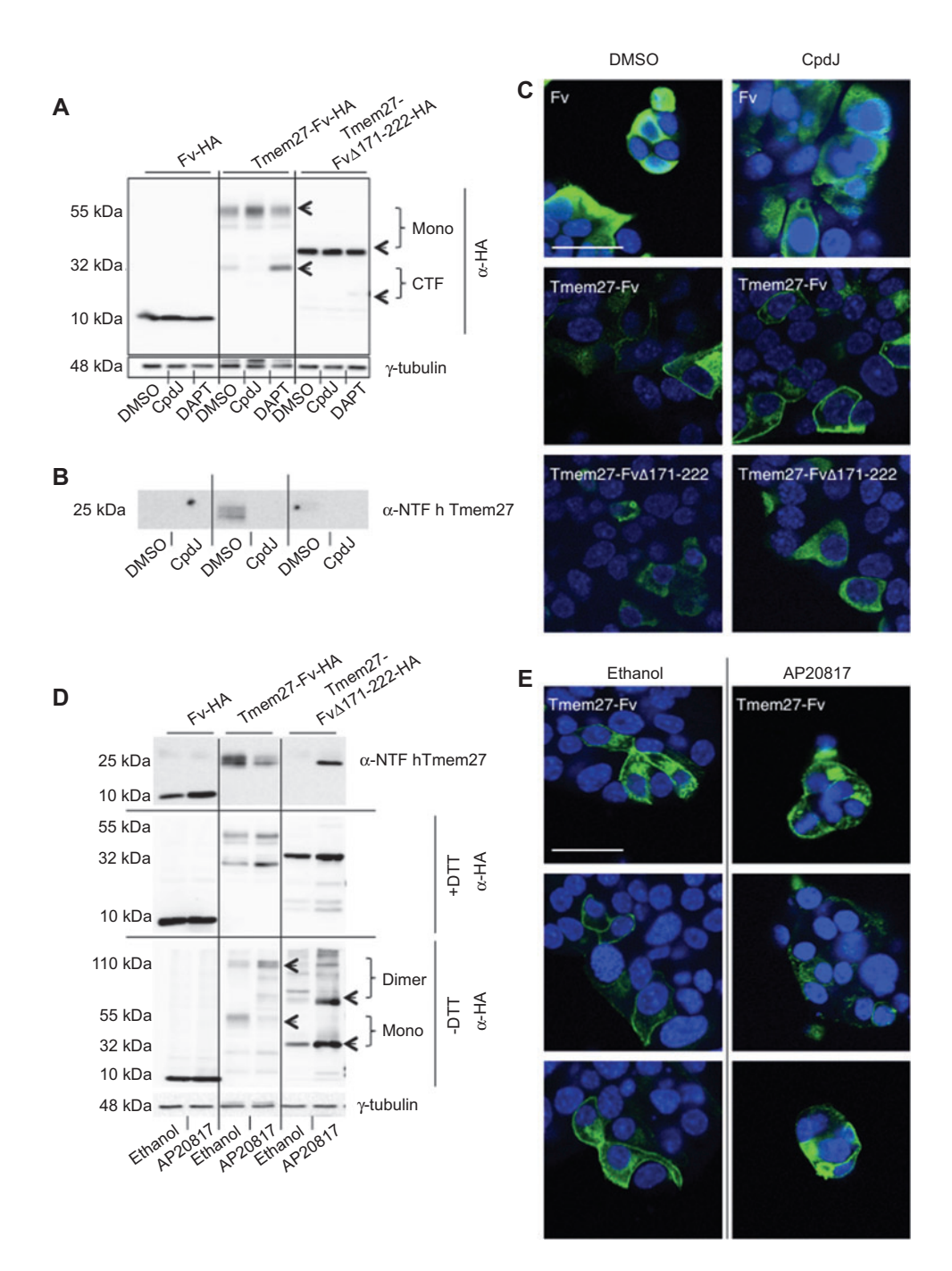


Figure 2 Inducing dimerization of hTmem27 by C-terminal fusion to human FK506-binding protein F36V (Fv) leads to decreased extracellular cleavage.

(A) Western blot (α -HA) for Fv only (10 kDa), hTmem27-Fv (55 kDa), or hTmem27 Δ 171-222-Fv (38 kDa) in lysates of MIN6 cells transfected with 5 μ g of respective plasmid/106 cells 24 h before 16-h treatment with 1 μ m DAPT, 200 nm CpdJ, or DMSO. Note that the hTmem27 Δ 171-222-Fv appears nonglycosylated and is cleavage defective. (B) Western blot for hTmem27 NTF in supernatant of MIN6 cells transfected with 5 μ g of respective plasmid/106 cells 24 h before 16-h treatment with 200 nm CpdJ or DMSO. (C) Immunofluorescence images of MIN6 cells transfected with 0.5 μ g of respective plasmid/106 cells 24 h before 16-h treatment with 200 nm CpdJ or DMSO, fixation, and staining for hTmem27 (α -HA). Bar=50 μ m. (D) Western blot for Fv only, hTmem27-Fv or hTmem27 Δ 171-222-Fv in supernatant (top blot, α -hTmem27 NTF) and lysates (middle blot, +DTT; bottom blot, -DTT; α -HA) of MIN6 cells transfected with 5 μ g of respective plasmid/106 cells 24 h before 12-h treatment with 1 nm AP20817 or ethanol vehicle. Note that the sharp bands in the supernatant from Fv only and hTmem27 Δ 171-222-Fv transfected cells are cytoplasmic contaminants that arise from the high levels of overexpression and stability of FL proteins and are recognized by the secondary antibody (α -mouse). Note also the additional bands at ~64 kDa and ~95 kDa in the AP20817 treated lane on -DTT blot, of which the 64-kDa band may correspond to forced dimers of CTF. (E) Immunofluorescence images of MIN6 cells transfected with 0.5 μ g of respective plasmid/106 cells 24 h before 12-h treatment with 1 nm AP20817 or ethanol vehicle, fixation, and staining for hTmem27 (α -HA). Three different frames are shown per condition to cover the spectrum of observed Tmem27 distributions. Bar=25 μ m.

N-linked glycosylation-deficient mutants of Tmem27 do not localize to the PM and are resistant to cleavage by Bace2

Given the recurrent observation that seemingly unglycosylated Tmem27 constructs mislocalized to non-cell surface

compartments and were poor Bace2 substrates, the importance of the two glycosylation sites in hTmem27, asparagine (N) 76 and N93 (Figure 3A) for localization and cleavage by Bace2 was investigated. Constructs were generated in which each N residue individually or in combination were mutated to isoleucine (I). All three, hTmem27_{N76I}, hTmem27_{N93I},

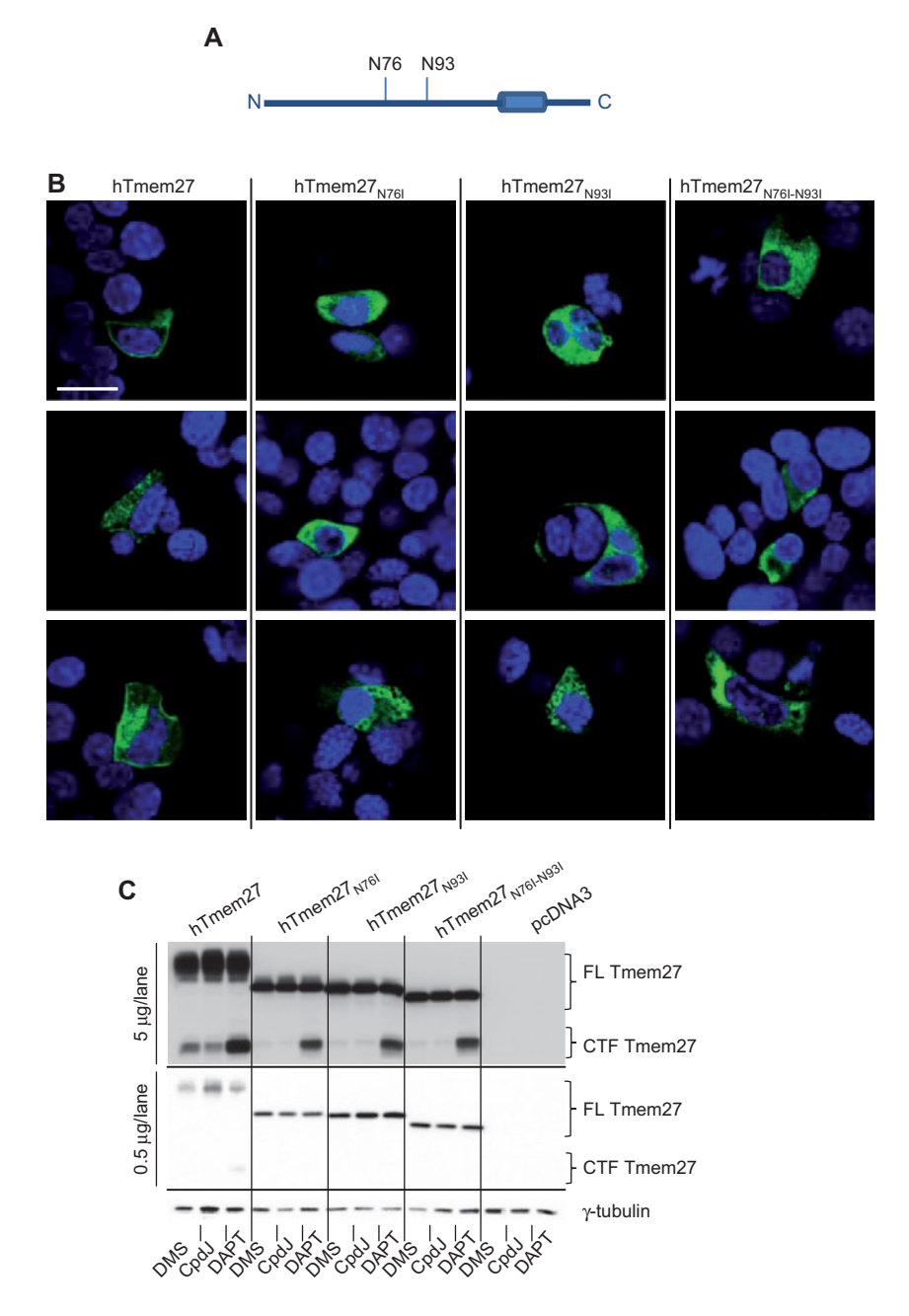


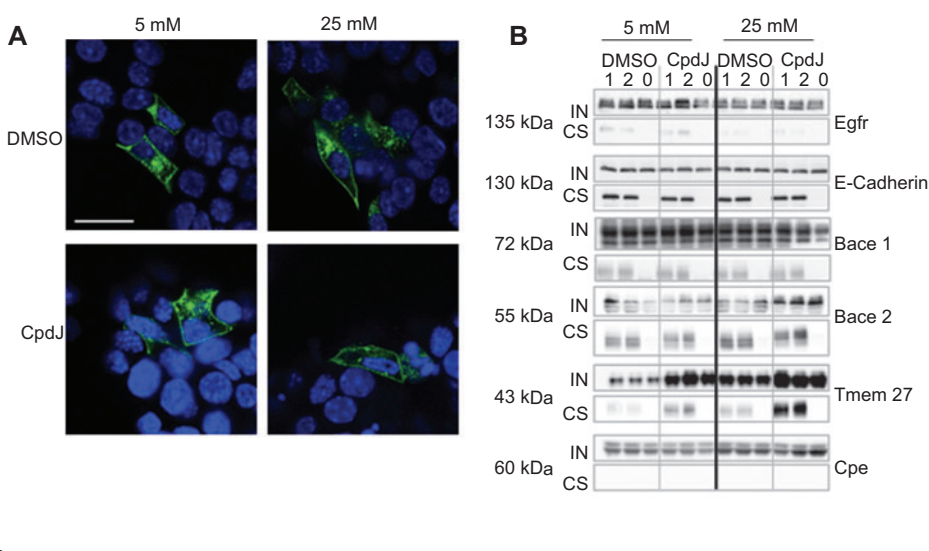
Figure 3 hTmem27 lacking of asparagine glycosylation is mislocalized to non-PM compartments and less susceptible to cleavage by Bace2.

(A) Schematic representation of hTmem27 showing positions of the two extracellular asparagine (N) residues that are predicted to be glycosylated. Numbers refer to hTmem27 amino acid residues (B) Immunofluorescence images of MIN6 cells transfected with 0.5 μ g of respective plasmid/10⁶ cells 24 h before fixation and staining for hTmem27 (α -V5). Three different frames are shown per mutant to cover the spectrum of observed Tmem27 distributions. Bar=25 μ m. (C) Western blot for hTmem27 (α -V5) in lysates of MIN6 cells transfected with 5 μ g of respective plasmid/10⁶ cells 24 h before 16-h treatment with 1 μ m DAPT, 200 nm CpdJ or DMSO. (Top) A total of 5 μ g protein was loaded on the top blot to detect the CTF of glycosylation-deficient mutants. (Bottom) A total of 0.5 μ g protein was applied per lane to detect expression difference between wild-type and mutant constructs as well as effects of CpdJ on FL Tmem27 levels.

hTmem27_{N76I-N93I}, were found to distribute to non-PM compartments when overexpressed in MIN6 (Figure 3B), similar to the hTmem27_{C75A} protein. Also, the proteins ran as sharp bands and at lower molecular weights than the wild-type construct on a Western blot (Figure 3C). Intriguingly, none was stabilized upon CpdJ incubation (Figure 3C, bottom), no NTFs were found in the supernatant (not shown), and only when high protein amounts were loaded could a CTF be observed upon DAPT addition (Figure 3C, top). These findings indicate that the loss of a single glycosylation is sufficient to cause Tmem27 mislocalization and prevent its cleavage.

Bace2 inhibition and high glucose lead to enrichment of Tmem27 at the PM

The emerging notion that targeting of Tmem27 to the PM is pivotal for its cleavage prompted us to study the localization of the protein under the two conditions known to induce increased Tmem27 protein levels: high glucose concentrations (Saisho et al., 2009) and Bace2 inhibition (Esterházy et al., 2011). Although it has been observed that the rate of Tmem27 degradation in MIN6 upon glucose stimulation is unaffected (Saisho et al., 2009) and that Bace2 inhibition truly leads to enzymatic inactivity (Esterházy et al., 2011), it



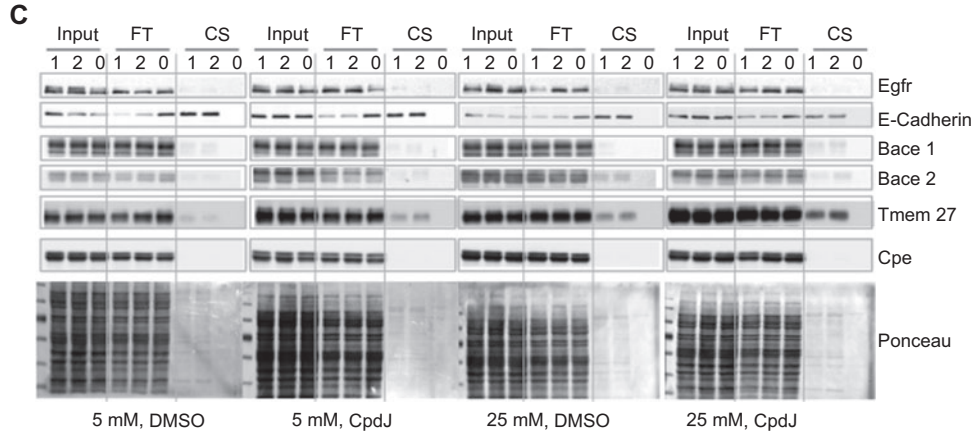


Figure 4 Increase of Tmem27 protein levels by Bace2 inhibition and high glucose leads to a proportional enrichment at the PM in MIN6 cells.

(A) Immunofluorescence images of MIN6 cells transfected with 0.5 μg of plasmid encoding hTmem27-V5/10⁶ cells 24 h before 16-h incubation with 200 nm CpdJ or DMSO in DMEM with low glucose (5 mm) or high glucose (25 mm), fixation, and staining for hTmem27 (α-V5). Bar=25 μm. (B) Western blot for Tmem27 and Bace2 and Bace1 in total cell lysates (IN) and cell surface (CS) fraction of MIN6 cells treated with 200 nm CpdJ or DMSO at 5 mm glucose or 25 mm glucose; 1 and 2 are biological duplicates of lysates from cells biotinylated on the surface before lysis and binding to Neutravidin beads; 0 represents lysate that originates from cells that were not treated with biotin. Ratio of IN/CS is 1:1. E-cadherin and EGFR were used as cell surface markers, Cpe as a non-PM marker. (C) Western blots for Tmem27 and Bace2 in total cell lysates (input), flow-through (FT), and cell surface (CS) fraction of MIN6 cells treated with 200 nm CpdJ or DMSO at 5 mm glucose or 25 mm glucose; 1 and 2 are duplicates of cells biotinylated on the surface before lysis and binding to Neutravidin beads; 0 indicates lysate from cells that were not treated with biotin. Ratio of IN/CS is 1:1 and IN/FT is 1:0.7. E-cadherin and EGFR were used as cell surface markers, Cpe as a non-PM marker. Ponceau of blots is shown at bottom to show loading levels.

is undetermined if Tmem27 also accumulates at the PM, the presumed compartment of its action (Akpinar et al., 2005). Conversely, it is currently unknown if these accumulation effects could additionally be explained by a sequestration from the cell surface and thereby protection from turnover. Staining of MIN6 cells expressing hTmem27 only revealed that, qualitatively, the protein still localized to the PM of MIN6 cells treated with high (25 mm) glucose or 200 nm CpdJ (Figure 4A). To quantitatively assess the amount of Tmem27 on the PM under these conditions, we used the live cell surface biotinylation technique, whereby before lysis, the cells are incubated on ice with impermeable, reactive biotin that covalently binds to primary amines in surface exposed protein and labeled molecules in the lysate are precipitated by Neutravidin conjugated beads. As expected, Tmem27 levels in the total MIN6 lysate increased upon 25 mm glucose compared with 5 mm glucose as well as upon CpdJ addition (Figure 4B, lane IN, Supplementary Figure 1). Only a fifth of the total lysate Tmem27 was found to be in the biotin-enriched fraction and thus cell surface (CS) at any given time (Figure 4B, C lanes CS), but this ratio was observed under all the conditions. Furthermore, Bace2 and Bace1 levels at the PM were unaffected by glucose and Bace inhibition, ruling out the alternative possibility that the proteases are sequestered (Figure 4B). Notably, the fraction of Tmem27 and Bace2 found at the surface was reminiscent of an intensely trafficking surface protein, the epidermal growth factor receptor (EGFR; Sorkin and Goh, 2008) (Figure 4B, C). The fact that only a portion of the total pool of these proteins was recovered in the cell surface fraction was furthermore not likely due to an inefficient biotinylation reaction, as 90% of E-cadherin, an important β -cell adhesion molecule (Dahl et al., 1996) of similar size as EGFR and therefore possessing similar amounts of primary amines, was precipitated (Figure 4B, C). Conversely, carboxypeptidase E (Cpe), an insulin granule resident transmembrane protein (Dhanvantari et al., 2002) that was up-regulated on the protein level upon high glucose in our system and against which a very strong antibody was available, was never found in the PM-enriched eluate, ruling out that the 10%-20% of Tmem27, Bace2, and EGFR recovered could be explained by unspecific binding of biotin to proteins in intracellular compartments or leaky cells (Figure 4B, C). These data show that enriching for total Tmem27 protein by high glucose and Bace2 inhibition does translate into increased amounts of the protein at the cell surface and that altered Tmem27 trafficking is not likely to contribute to the stabilizing effects.

Mutating the extracellular cleavage site including the Phe-Phe motif renders Tmem27 more susceptible to Bace2 cleavage at the membrane proximal cleavage site

Three Bace2 cleavage sites in hTmem27 have been identified by mass spectrometry (Esterházy et al., 2011), two clustered sites after phenylalanine (F) 116 and leucine (L) 118 (area A, in blue, Figure 5A), giving rise to CTF A1 and CTF A2, respectively (Figure 5A), and one more membrane proximal

site at F125, giving rise to CTF B (area B, in red, Figure 5A). The existence of multiple cleavage sites could serve several purposes: first, it could be a simple safeguard mechanism to ensure removal of a protein; second, the sites may synergize or antagonize cleavage at a particular site as 'intramolecular competitive antagonists'; third, the alternative cleavage products arising could possess different biological activities. To elucidate the role of cleavage site areas A and B in hTmem27 processing by Bace2, each region was mutated on its own or in combination to either multiple glycines (G), multiple alanines (A), or a stretch of amino acids with large side chains of different charges or sizes from the wild-type residues at the same position (115-119 TYYLR instead of AFFLN in area A and 123-128 NTYGKR instead of LEFLKI in area B). Of note, our previous attempts to mutate single residues to amino acids as diverse as alanine, glycine, tryptophan, or aspartic acid failed to induce any change in hTmem27 cleavage (data not shown). Independently of the residues introduced in area A (115-118G, 114-119A, 115-119TYYLR), mutation of this region led to a marked enrichment of a CTF upon DAPT treatment that exhibited similar electrophoretic mobility as the wild-type CTF, indicating accelerated processing by Bace2 (Figure 5B). This coincided with reduced levels of the FL protein compared with wild type, as would be expected for a protein that is more susceptible to cleavage; however, all of these gross mutations led to lower expression levels compared with wild type, probably due to misfolding and also to apparent glycosylation defects (Figure 5B, Supplementary Figure 2). Therefore, the ratio of CTF to FL protein was used to determine whether cleavage was affected in the mutants. Indeed, Figure 5C shows that area A mutants displayed a 1.2- to 2-fold increase in the CTF/FL ratio compared with wild type. In contrast, mutating area B to G (123-126G) led to the appearance of a weaker CTF band that also ran at a higher molecular weight than the wild-type CTF and therefore probably reflected a shift toward cleavage in area A that gives rise to CTF A1/2 (Figure 5B, C). This shift also indicated that the enriched, lower molecular weight band in the area A mutants represented CTF B, which is likely the naturally preferred Bace2 cleavage site, as it was the same size as wild-type CTF. Mutating area B to 123-126A or 123-128NTYGR did not have such pronounced effects on CTF generation (Figure 5B, C). However, when both areas A and B were mutated in a single construct (115-118G, 123-126G or 114-119A, 123-126A or 115-119 TYYLR, 123-128 NTYGKR), the CTF/FL ratio was also decreased in the latter two (Figure 5C), and the FL protein reached almost wildtype levels (Supplementary Figure 2). Furthermore, the CTF ran as a more diffuse band at a size close to that expected upon cleavage in area A (Figure 5B).

In addition to the ratio of CTF/FL protein, two further readouts can be used to determine the efficiency of Tmem27 processing by Bace2: the stabilization of the FL protein upon Bace2 inhibition in the cell lysate and the level of its shed NTF in the supernatant. The quantification of the FL ratio of the mutants in the presence of CpdJ compared with DMSO and its normalization to the wild-type CpdJ/DMSO ratio revealed that although area A mutants in this assay behaved

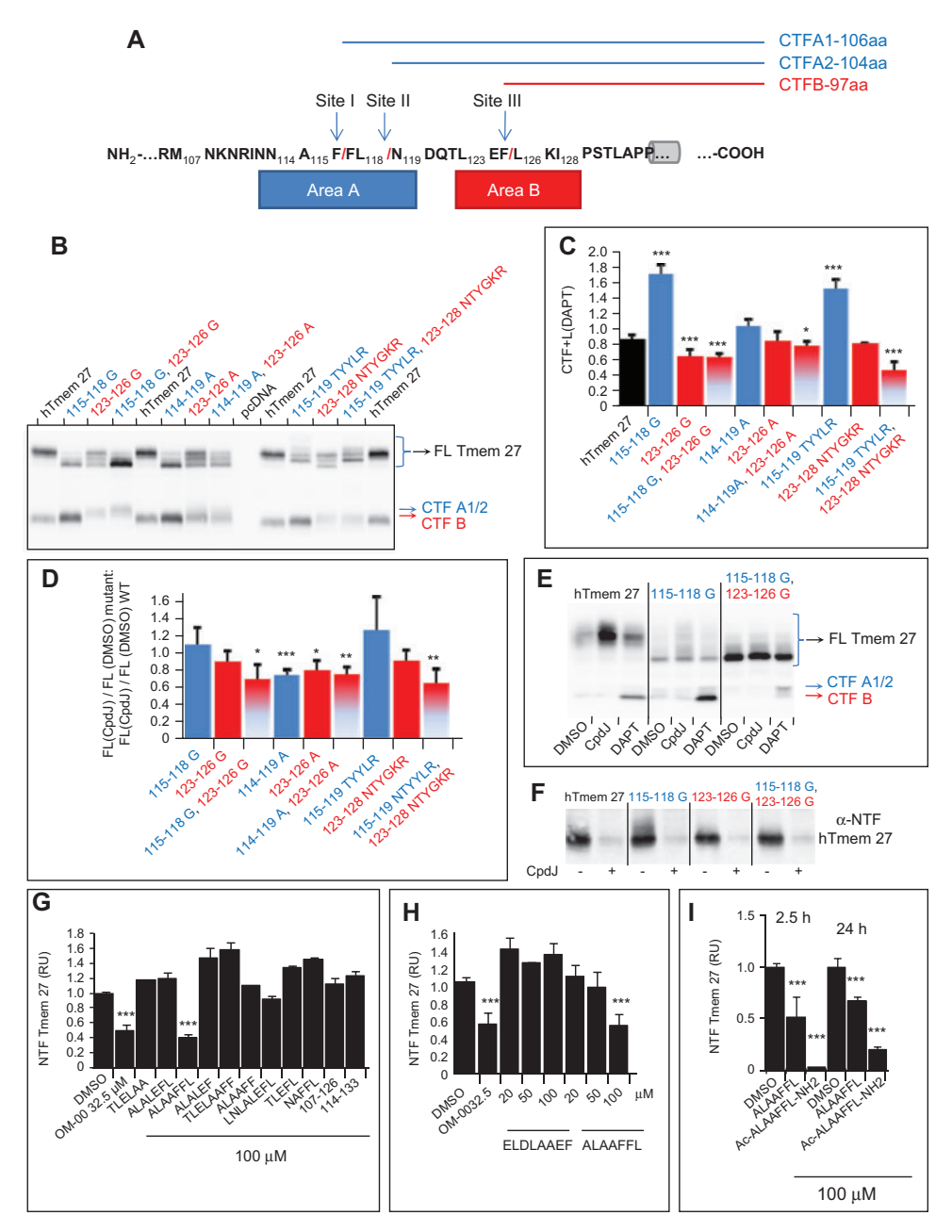


Figure 5 The cleavage site region of Tmem27 containing the Phe-Phe motif acts as a negative regulator of shedding by Bace2. (A) Schematic representation of the extracellular juxtamembrane domain of hTmem27. Cleavage sites I and II in area A (blue) and site II in area B (red) are indicated. Numbers in sequence refer to amino acid residues in hTmem27 that are mentioned throughout this figure. The CTFs arising from respective cleavages are sketched on top of sequence as CTF A1/2 (blue) and B (red). Numbers next to CTFs refer to total amino acid length of CTFs. Gray cylinder represents transmembrane domain (residues 142–164). (B) Western blot for hTmem27 (α-V5) and its indicated mutant forms in cell lysate of MIN6 cells transfected with 5 μg of respective plasmid/106 cells 24 h before 16-h treatment with 1 μm DAPT. Mutants and CTFs representing cleavage in area A are indicated blue, in area B in red, an in both blue and red. (C) Quantification of ratio of CTF to FL hTmem27 and indicated mutants after a 16-h treatment with 1 µm DAPT. Western blots with biological triplicates were quantified. Note that the ratio of FL to CTF in the cell lysate rather than the ratio of FL in cell lysate to N-terminal fragment (NTF) in the supernatant was used to determine cleavage efficiency because this ratio can be quantified within a single sample, thus avoiding falsifications that arise from cross-blot comparisons. (D) Quantification of ratio of FL mutant hTmem27 treated with 200 nm CpdJ to FL levels upon DMSO treatment, normalized to the ratio of wild-type hTmem27 treated with 200 nm CpdJ to DMSO. Western blots from three independent experiments were quantified. (E) Example Western blot for hTmem27 (α-V5) in lysates of MIN6 cells transfected with 5 μg of respective plasmid/10⁶ cells 24 h before 16-h treatment with 1 µm DAPT, 200 nm CpdJ, or DMSO that was used to quantify ratios in (D). (F) Western blot for the NTF of hTmem27 (mAb 1/33) in supernatant of MIN6 cells transfected with 5 µg of respective plasmid/106 cells 24 h before 16-h treatment with 200 nm CpdJ or DMSO. (G) Quantification of shed Tmem27 in supernatant from MIN6 cells treated with 100 μm of indicated peptide, 2.5 μm OM-003 (H-ELD-[(2R,4S,5S)-5-amino-4hydroxy-2,7,-dimethyl-octanyl-]-AEF-OH) or DMSO for 2.5 h and detected with anti-N-terminal

Tmem27 antibody (coll3). Note that epitope for coll3 is mouse amino acid residue 101-120. Signal intensities were normalized to DMSO signal and are expressed as relative units (RU). (H) Quantification of shed Tmem27 in supernatant from MIN6 cells treated with $20-100~\mu m$ of peptide ELDLAAEF, the nontransition mimetic from of OM-003, $2.5~\mu m$ of OM-003, or DMSO for 2.5~h and detected with coll3 antibody. Signal intensities were normalized to DMSO signal and are expressed as relative units (RU). (I) Quantification of shed Tmem27 in supernatant from MIN6 cells treated with $100~\mu m$ of peptide ALAAFFL, Ac-ALAAFFL-NH₂, or DMSO for 2.5~h (left) or 24~h (right) detected with coll3 antibody. Signal intensities were normalized to the DMSO signal at each time point and are expressed as relative units (RU). Data represent means $\pm SD$; * $p \le 0.05$, ** $p \le 0.01$, *** $p \le 0.001$.

almost like wild type (except for 114-119A), area B and area A/B double mutants were only stabilized by 60% compared with nonmutated hTmem27 (Figure 5D, E). Given the altered apparent molecular weight of the cleavage site mutants on Western blots, one concern was that this pattern was a consequence of altered glycosylation, which could lead to protein mislocalization and thus prevention of hTmem27 cleavage in the area B and area A/B double mutants. However, all the mutants localized at least partially to the PM in MIN6 cells (Supplementary Figure 3), similar to the wild-type constructs (Figure 1D, Figure 2B). Monitoring the NTF in the supernatant of MIN6 cells revealed that area A mutants displayed an enrichment in this fragment, as is expected for higher-affinity Bace2 substrates, whereas the supernatant of area B and area A/B mutants generated less NTF than the wild-type sample (Figure 5F, showing the G mutant series). Loss of the NTF upon Bace2 inhibition revealed that, in all cases, the shed fragment disappeared to a similar degree as in the wild-type supernatant, indicating that although the mutants displayed altered cleavage rates, their main protease remained to be Bace2 (Figure 5F).

Although the instability of the FL cleavage site mutants precluded any further functional analyses, the observation that the mutation of the Phe-Phe containing site in hTmem27 led to increased shedding implied that this sequence could reduce Bace2 activity and could be exploited. In fact, the first generation of Bace1 inhibitors was based on amyloid precursor protein (APP) cleavage site peptides, such as the APP transition state analogue OM-003 (John et al., 2003), which is based on the M671L mutant form of APP ('Swedish mutant' causing familial Alzheimer disease; Mullan et al., 1992). To assess the potential of a Phe-Phe-containing peptide for Bace2 inhibition, several 5- to 7-amino acid long peptides containing this motif were designed. The flanking amino acids were varied to increase the probability that one peptide would be able to penetrate into the cell, as cell impermeable Bace inhibitors are not able to inhibit Bace2 (Esterházy et al., 2011). Control peptides were also included and were based on area B and longer peptides stretching from residue 107 to 126 or 114 to 133 (Figure 5A). The supernatant of MIN6 cells was analyzed for endogenous Tmem27 NTF using an antibody raised against peptide 101-120 (coll3). No effect on NTF levels was observed after 24 h, but after a 2.5-h treatment with 100 µm of the peptides, one peptide, ALAAFFL, satisfied the requirements for Bace2 inhibition and decreased shed Tmem27 levels to the same degree as 2.5 µm of OM-003 (Figure 5G, Supplementary Figure 4A). Compared with synthetic Bace inhibitors, this was a weak and transient effect that also did not translate into FL Tmem27 stabilization in the cell lysate (data not shown); however, it was much more effective in decreasing the NTF signal than the nontransition state equivalent of OM-003, ELDLAAEF (Figure 5H, Supplementary Figure 4B). Furthermore, rendering the peptide ALAAFFL more permeable and stable by N-terminal acetylation and C-terminal amidation increased its efficiency and prolonged its effect to 24 h (Figure 5I, Supplementary Figure 4C). Of note, the decrease in Tmem27 shedding upon Ac-ALAAFFL-NH, was also detected with an anti-Tmem27 N-terminus antibody raised against Tmem27 peptide 29-46 (Supplementary Figure 4D, E), excluding the possibility that the perceived inhibitory effect was in reality due to an epitopemasking effect. Protection of peptides by acetylation and amidation conferred Tmem27 inhibitory activity to further AFFL containing peptides; however, none reached the efficacy of Ac-ALAAFFL-NH, after 2.5 or 24 h (Supplementary Figure 4F, G).

In summary the data suggest that the preferred Bace2 cleavage site within hTmem27 is between F125 and L126 in area B, but area A acts as an alternative site, especially when area B is mutated. Furthermore, area A, which contains the double phenylalanine (Phe-Phe) motif, acts as an intramolecular competitive antagonist that reduces cleavage efficiency in area B, even when applied exogenously as a peptide.

Discussion

The data described here show that the Tmem27 amino acid sequence harbors essential information for its dimerization, glycosylation, localization, and processing by Bace2. Of the three cysteines, the intracellular residue appears most essential for mediating Tmem27 dimerization, as mutating it to alanine abolishes dimer formation. The dependence of this oligomerization state on an intracellular cysteine is less frequent than the involvement of extracellular residues because the cytosolic environment is usually reducing and thus does not favor disulfide bond formation. However, other transmembrane proteins such as the MUC1 oncoprotein (Leng et al., 2007) and the vaccinia virus A17L envelope protein (Betakova and Moss, 2000) have been shown to dimerize via intracellular cysteines. Given that endogenous Tmem27 appears as dimers as much as monomers, this mechanism may further indicate that the protein resides in cellular microenvironments with a low cytosolic reduction potential. We have applied various metabolic stress conditions to MIN6 cells to elucidate whether they would alter the ratio of monomer to dimer (unpublished data), but none translated into a shift in the balance, as shown by Western blotting. This is in line with the observation that Tmem27 stabilization by Bace2 inhibition leads to enrichment of both forms and hence the equilibrium between the two states is very dynamic. On the other hand, induced dimerization of Tmem27 leads to the reduction of its cleavage, suggesting that the dimer is not a substrate for Bace2. Interestingly, the Bace substrate APP homodimerizes as well (Scheuermann et al., 2001) and its forced dimerization also abolishes cleavage and thereby toxic $A\beta$ production by the protease Bace1 (Eggert et al., 2009), the close homologue of Bace2, indicating that substrate cleavage regulation by dimerization is a more general paradigm. Clearly, more work is needed in the future to identify situations in which cellular oxidation states and/or dimerization of these proteins are altered.

Proper glycosylation of Tmem27 is important for its cell surface localization, as the glycosylation-deficient mutants accumulate in other compartments. It should be noted that the primary cause for lack of glycosylation and therefore proper localization within the cell may, in principle, also be misfolding of mutant hTmem27 (C75A and hTmem27-Δ171-222-Fv-HA) that prevents the access of glycosyltransferases to the protein. However, these mutants were at the same time more stable than wild-type hTmem27, suggesting they were not subjected to unfolded protein response pathways. Either way, the fact that they are at the same time poor Bace2 substrates suggests that the PM is a critical compartment for substrate and protease interaction, although not necessarily cleavage (which is thought to also occur in early endosomal vesicles derived from the PM that fuse back with the cell surface after catalysis; Walter, 2006). PM is also a compartment of mature Bace2, as unless the protease is inhibited, only mature Bace2 was found at the cell surface in the biotinylation experiment, as previously described by Fluhrer et al. (2002). The sugar side chains are not very likely to be important for the interaction between Tmem27 and Bace2 once the proteins are in the same compartment because the area A mutants that appear partially glycosylation deficient are very good Bace2 substrates. The importance of Tmem27 glycosylation in its targeting to the PM, the compartment in which it is likely to exert its proliferative action, may also have implications on the protein's function in conditions of β -cell dysfunction: free fatty acids have recently been reported to induce the downregulation of a crucial N-glycosyltransferase, GnT-4a, which results in reduced Glut2 glycosylation and hence decreased cell surface expression and glucose-stimulated insulin secretion (Ohtsubo et al., 2011). Conceivably, Tmem27 glycosylation defects induced by the metabolic environment could impair its function and thereby contribute to the β -cell demise in type 2 diabetes in a similar manner.

Bace2 inhibition and high glucose have been shown to increase Tmem27 protein in MIN6 cells independently of transcription but rather by decreasing turnover (Esterházy et al., 2011) and possibly accelerating translation (Saisho et al., 2009), respectively. Here we, for the first time, show that these increases in total Tmem27 protein levels do translate into elevated cell surface concentrations as well. The level of Tmem27 at the PM remains proportional to its total levels upon glucose stimulation or Bace2 inhibition, suggesting that the Tmem27-trafficking machinery – which is likely to carry other cargos as well - is not affected. This is a significant finding given that other conditions (such as lack of glycosylation) can lead to Tmem27 accumulation, yet in an inappropriate compartment.

The existence of multiple proximal cleavage sites has also been observed for Bace 1/2 substrates other than Tmem 27 (Sun et al., 2006; Kuhn et al., 2007; Hogl et al., 2011), indicating that this is a more common feature. The substrate cleavage sequence has also been shown to affect shedding efficiency, the best studied example being the familial APP M671L Swedish mutant at the cleavage site between residues 671 and 672 that leads to a substantially increased turnover by Bace1 and therefore toxic $A\beta$ production (Mullan et al., 1992). Mutations in the cleavage region that lead to decreased APP or other substrate processing by Bace1 have not been reported, and naturally occurring ones are probably difficult to find by phenotyping. Intriguingly, another rare APP mutant that leads to late onset familial Alzheimer disease is A692G (Flemish mutant; Hendriks et al., 1992), which prevents α-secretases such as Adam10 and Adam17 from cleaving between Phe690 and Phe691 (the ' θ site'; Sun et al., 2006), and therefore leads to reduced competition for the substrate with Bace1 that can cleave more efficiently at the β -secretase site (Lichtenthaler, 2011). Bace2 itself is in fact capable of cutting APP at this Phe690-Phe691 site and therefore acting as a θ -secretase (Fluhrer et al., 2002; Sun et al., 2006), but given its low cerebral expression, Bace2 is not likely to contribute a Bace1antagonizing effect in the brain. Although the Phe-Phe doublet in Tmem27 competes for the same protease, Bace2, that cuts at the preferred Tmem27 site (Phe125-Leu126) as well, whereas in APP this sequence leads to the competition of two different protease classes for the substrate (α-secretases cleaving between Phe690 and Phe691, Bace1 cleaving between Met671 andAsp672), the net effect in both cases is that the motif slows down processing of the FL proteins and thereby contributes to their stability. A juxtamembrane Phe-Phe motif may also be a potent predictor of a Bace2 cleavage site, even if the cleavage at other, less well-defined signatures, appears to be more efficient. Although the Phe125-Leu126 site in Tmem27 is conserved across most vertebrates (Supplementary Figure 5A), the Phe116-Ph117 is replaced by Phe116-Leu117 in phyla more distally related to mammals, such as birds, amphibians, and fish, giving rise to the speculative idea that slowing Bace2 activity by a Phe-Phe motif in its target only became advantageous later in evolution. The 30-amino acid N-terminal of the Tmem27 transmembrane domain that contain the cleavage sites displays a similar phylogenetic relatedness as the entire Tmem27 sequence (Supplementary Figure 5B, C), as does the protein sequence of Bace2 (not shown), supporting the concept that selective pressure to adjust to the protease, substrate, or terrestrial environment existed.

Finally, small synthetic molecules that mimic the critical properties of the Phe-Phe motif may be promising candidates for more Bace2-selective inhibitors than the compounds so far characterized, which all inhibit Bace1 as well. In summary, the multiple mechanisms by which the intramolecular motifs in Tmem27 determine its localization and processing by Bace2 suggest that they have evolved to ensure the tight and dynamic regulation of this protein's action and thus β -cell mass.

Materials and methods

Protease inhibitors and peptides

Merck BACE inhibitor IV (MerckBI) was purchased from Calbiochem (Darmstadt, Germany); γ -secretase inhibitor DAPT from Sigma (Munich, Germany); CpdJ was synthesized by Roche (Basel, Switzerland), according to previous descriptions (Esterházy et al., 2011); OM-003 was obtained from Bachem (Bubendorf, Switzerland). Unmodified peptides were custom synthesized by Apara Bioscience (Denzlingen, Germany). N-acetylated and C-amidated peptides were generated by Peptide 2.0 (Chantilly, VA, USA).

Antibodies

The antibodies against N-terminal Tmem27 was rabbit coll3 (raised against mouse Tmem27 101-120, used at 1:500; Bethyl Laboratories, Montgomery, TX, USA) or mouse anti-Tmem27 2G5 (raised against mouse Tmem27 29-46, used at 1:500; Enzo Life Sciences, Plymouth Meeting, PA, USA), and C-terminal Tmem27 was rabbit coll4 (raised against mouse Tmem27 194-214, used at 1:500, Bethyl Laboratories) as described previously (Akpinar et al., 2005; Danilczyk et al., 2006). The other antibodies used for immunoblotting (IB) and immunohistochemistry (IHC) were used in the following dilutions and purchased from the following companies: mouse anti-V5 (1:5000 IB, 1:500 IHC; Invitrogen, Grand Island, NY, USA), mouse anti-HA (1:1000 IB, 1:100 IHC; Covance, Berkeley, CA, USA), mouse anti- β -tubulin (1:6000; Sigma), rabbit anti-E-cadherin (1:2500; Cell Signaling, Danvers, MA, USA), rabbit anti-EGFR (1:1000; Cell Signaling), rabbit anti-Bace1 (1:2000; Epitomics, Burlingame, CA, USA), goat anti-Bace2 (1:500; Santa Cruz, CA, USA), mouse anti-Cpe (1:3000; BD Transduction Laboratories, Heidelberg, Germany). Mouse anti-NTF hTmem27 (antibody mAb1/33, 1:500) was a gift from F. Hoffmann-La Roche (Basel, Switzerland). Secondary antibodies were obtained from Calbiochem (horseradish peroxidase linked for IB, 1:10 000) or Invitrogen (ALEXA fluor labeled for IHC, 1:500).

Other reagents

The pC4-Fv1E plasmid and dimerizer AP20817 were obtained as part of the ARGENT regulated homodimerization kit (ARIAD, Cambridge, MA, USA). The biotinylation based cell surface protein isolation kit was purchased from Pierce (Rockford, IL, USA) (Cat. No 89881).

Cell culture

MIN6 cells were maintained in DMEM (Gibco, Darmstadt, Germany) containing 25 mm glucose, 15% FBS, 55 μm β -mercaptoethanol and penicillin/streptomycin.

Cloning

The template for the hTmem27 mutants was hTmem27 in pcDNA3.1-His6V5-TOPO vector (Invitrogen; Akpinar et al., 2005), and the constructs were generated using a PCR approach. Mutant hTmem27 was exchanged against the wild-type hTmem27 in the pcDNA3.1-His6V5-TOPO backbone by restriction enzyme digest. For the inducible dimers, hTmem27 was cloned into the pC4-Fv1E vector (ARIAD) using a PCR approach. All mutations were confirmed by DNA sequencing.

Transient transfection with plasmids

MIN6 cells were either transfected with 5 μ g DNA/106 cells by electroporation in AMAXA nucleofector V solution (Lonza, Cologne, Germany) using manufacturer's single-cuvette electroporator and programme G-016 (available online at www.amaxa.com) for cell lysate analysis or 0.5 μ g DNA/106 cells using Lipofectamine 2000 (Invitrogen) for immunofluorescent image analyses of the constructs.

Protease inhibition

MIN6 cells were incubated with 5 μ m Merck Bace inhibitor IV (MerckBI), 1 μ m DAPT, and 200 nm of CpdJ for 6–16 h in Opti-mem (Gibco), except for the cell surface biotinylation experiment, which was performed in serum-free DMEM (Gibco). OM-003 was used at 2.5 μ m, and the Tmem27-based peptides at 20–100 μ m for 2.5–24 h.

Immunoblotting

Whole cell protein extracts were boiled in Laemmli buffer, separated by SDS-PAGE (10%, 12%, or 15%) and transferred to a nitrocellulose membrane by electroblotting. Supernatants were either subjected to SDS-PAGE or left in the native state and transferred to a nitrocellulose membrane by hydraulic pressure using a 48-well SlotBlot (BioRad, USA). All primary antibodies were used in TBS-0.1% Tween 20 (Sigma) with 5% fat-free milk, except for anti-EGFR and anti-E-cadherin for which the milk was replaced by 3% BSA and the membranes were incubated overnight at 4°C. Secondary antibodies were binding for 1 h at room temperature. Signal intensities were quantified using the Fuji Multi Gauge software.

Immunofluorescence

MIN6 cells were grown on Nunc Delta surface culture plates (Nunc, Roskilde, Denmark), fixed in 3.7% formaldehyde, permeabilized in PBS-0.2% saponin (Sigma) and blocked in PBS-0.2% saponin with 3% BSA. Primary antibodies were applied in blocking buffer overnight at 4°C, secondary antibodies for 1 h at room temperature. Images were captured using a Leica TCS SPE confocal microscope (Heerbrugg, Switzerland).

Cell surface biotinylation

Cell surface biotinylation was performed according to the manufacturer's protocol (Pierce, USA).

Bioinformatics

Protein sequences from different species were retrieved using the Basic Local Alignment Search Tool provided by the National Center for Biotechnology information (NCBI). Evolutionary analyses were conducted using MEGA5 software that is available online for use in research (www.megasoftware.net). The program infers evolutionary history using the unweighted pair group method with arithmetic mean (UPGMA) method and computes evolutionary distances using the Poisson correction method.

Statistical analysis

All data were analyzed using a two-tailed Student's *t*-test and rejecting the null hypothesis at p=0.05. Data represent means \pm standard deviation (SD), *p<0.05, **p<0.01, ***p<0.001.

Acknowledgements

This work was in part funded by the Juvenile Diabetes Research Foundation International. We thank ARIAD for providing the ARGENT regulated homodimerization kit (F. Hoffmann-La Roche, Basel, Switzerland), for CpdJ, Dr. Hugues Matile (F. Hoffmann-La Roche) for providing anti-NTF hTmem27 antibody mAb 1/33, and Dr. Heinz Döbeli (F. Hoffmann-La Roche) for fruitful discussions.

References

- Akpinar, P., Kuwajima, S., Krutzfeldt, J., and Stoffel, M. (2005). Tmem27: a cleaved and shed plasma membrane protein that stimulates pancreatic β cell proliferation. Cell Metab. 2, 385–397.
- Betakova, T. and Moss, B. (2000). Disulfide bonds and membrane topology of the vaccinia virus A17L envelope protein. J. Virol. 74, 2438–2442.
- Dahl, U., Sjodin, A., and Semb, H. (1996). Cadherins regulate aggregation of pancreatic β -cells *in vivo*. Development *122*, 2895–2902.
- Danilczyk, U., Sarao, R., Remy, C., Benabbas, C., Stange, G., Richter, A., Arya, S., Pospisilik, J.A., Singer, D., Camargo, S.M., et al. (2006). Essential role for collectrin in renal amino acid transport. Nature 444, 1088–1091.
- Dhanvantari, S., Arnaoutova, I., Snell, C.R., Steinbach, P.J., Hammond, K., Caputo, G.A., London, E., and Loh, Y.P. (2002). Carboxypeptidase E, a prohormone sorting receptor, is anchored to secretory granules via a C-terminal transmembrane insertion. Biochemistry 41, 52–60.
- Eggert, S., Midthune, B., Cottrell, B., and Koo, E.H. (2009). Induced dimerization of the amyloid precursor protein leads to decreased amyloid- β protein production. J. Biol. Chem. 284, 28943–28952.
- Esterházy, D., Stutzer, I., Wang, H., Rechsteiner, M.P., Beauchamp, J., Dobeli, H., Hilpert, H., Matile, H., Prummer, M., Schmidt, A., et al. (2011). Bace2 is a β cell-enriched protease that regulates pancreatic beta cell function and mass. Cell Metab. *14*, 365–377.
- Fluhrer, R., Capell, A., Westmeyer, G., Willem, M., Hartung, B., Condron, M.M., Teplow, D.B., Haass, C., and Walter, J. (2002). A non-amyloidogenic function of BACE-2 in the secretory pathway. J. Neurochem. 81, 1011–1020.
- Hendriks, L., van Duijn, C.M., Cras, P., Cruts, M., Van Hul, W., van Harskamp, F., Warren, A., McInnis, M.G., Antonarakis, S.E., Martin, J.J., et al. (1992). Presentle dementia and cerebral haemorrhage linked to a mutation at codon 692 of the β-amyloid precursor protein gene. Nat. Genet. 1, 218–221.
- Hogl, S., Kuhn, P.H., Colombo, A., and Lichtenthaler, S.F. (2011). Determination of the proteolytic cleavage sites of the amyloid precursor-like protein 2 by the proteases ADAM10, BACE1 and γ-secretase. PLoS One 6, e21337.

- Jin, L., Zeng, H., Chien, S., Otto, K.G., Richard, R.E., Emery, D.W., and Blau, C.A. (2000). *In vivo* selection using a cell-growth switch. Nat. Genet. 26, 64–66.
- John, V., Beck, J.P., Bienkowski, M.J., Sinha, S., and Heinrikson, R.L. (2003). Human α-secretase (BACE) and BACE inhibitors. J. Med. Chem. 46, 4625–4630.
- Kahn, S.E., Hull, R.L., and Utzschneider, K.M. (2006). Mechanisms linking obesity to insulin resistance and type 2 diabetes. Nature 444, 840–846.
- Kuhn, P.H., Marjaux, E., Imhof, A., De Strooper, B., Haass, C., and Lichtenthaler, S.F. (2007). Regulated intramembrane proteolysis of the interleukin-1 receptor II by α -, β -, and γ -secretase. J. Biol. Chem. 282, 11982–11995.
- Leng, Y., Cao, C., Ren, J., Huang, L., Chen, D., Ito, M., and Kufe, D. (2007). Nuclear import of the MUC1-C oncoprotein is mediated by nucleoporin Nup62. J. Biol. Chem. 282, 19321–19330.
- Lichtenthaler, S.F. (2011). Alpha-secretase in Alzheimer's disease: molecular identity, regulation and therapeutic potential. J. Neurochem. 116, 10–21.
- Mullan, M., Crawford, F., Axelman, K., Houlden, H., Lilius, L., Winblad, B., and Lannfelt, L. (1992). A pathogenic mutation for probable Alzheimer's disease in the APP gene at the N-terminus of β-amyloid. Nat. Genet. 1, 345–347.
- Ohtsubo, K., Chen, M.Z., Olefsky, J.M., and Marth, J.D. (2011). Pathway to diabetes through attenuation of pancreatic beta cell glycosylation and glucose transport. Nat. Med. *17*, 1067–1075.
- Saisho, K., Fukuhara, A., Yasuda, T., Sato, Y., Fukui, K., Iwahashi, H., Imagawa, A., Hatta, M., Shimomura, I., and Yamagata, K. (2009). Glucose enhances collectrin protein expression in insulin-producing MIN6 β cells. Biochem. Biophys. Res. Commun. 389, 133–137.
- Scheuermann, S., Hambsch, B., Hesse, L., Stumm, J., Schmidt, C., Beher, D., Bayer, T.A., Beyreuther, K., and Multhaup, G. (2001). Homodimerization of amyloid precursor protein and its implication in the amyloidogenic pathway of Alzheimer's disease. J. Biol. Chem. 276, 33923–33929.
- Sorkin, A. and Goh, L.K. (2008). Endocytosis and intracellular trafficking of ErbBs. Exp. Cell Res. *314*, 3093–3106.
- Sun, X., He, G., and Song, W. (2006). BACE2, as a novel APP theta-secretase, is not responsible for the pathogenesis of Alzheimer's disease in Down syndrome. FASEB J. 20, 1369–1376.
- Walter, J. (2006). Control of amyloid- β -peptide generation by subcellular trafficking of the β -amyloid precursor protein and β -secretase. Neurodegener. Dis. 3, 247–254.

Received January 10, 2012; accepted February 4, 2012